

d-TreeRPO: Towards More Reliable Policy Optimization for Diffusion Language Models

Leyi Pan^{1,2*}, Shuchang Tao², Yunpeng Zhai², Zheyu Fu¹, Liancheng Fang³, Minghua He⁴, Lingzhe Zhang⁴, Zhaoyang Liu², Bolin Ding², Aiwei Liu^{1†}, Lijie Wen^{1†}

¹Tsinghua University, ²Tongyi Lab, Alibaba Group,

³University of Illinois at Chicago, ⁴Peking University

panly24@mails.tsinghua.edu.cn, liuaiwei12@gmail.com, wenlj@tsinghua.edu.cn

Abstract

Reliable reinforcement learning (RL) for diffusion large language models (dLLMs) requires both accurate advantage estimation and precise estimation of prediction probabilities. Existing RL methods for dLLMs fall short in both aspects: they rely on coarse or unverifiable reward signals, and they estimate prediction probabilities without accounting for the bias relative to the true, unbiased expected prediction probability that properly integrates over all possible decoding orders. To mitigate these issues, we propose *d*-TreeRPO, a reliable RL framework for dLLMs that leverages tree-structured rollouts and bottom-up advantage computation based on verifiable outcome rewards to provide fine-grained and verifiable step-wise reward signals. When estimating the conditional transition probability from a parent node to a child node, we theoretically analyze the estimation error between the unbiased expected prediction probability and the estimate obtained via a single forward pass, and find that higher prediction confidence leads to lower estimation error. Guided by this analysis, we introduce a time-scheduled self-distillation loss during training that enhances prediction confidence in later training stages, thereby enabling more accurate probability estimation and improved convergence. Experiments show that *d*-TreeRPO outperforms existing baselines and achieves significant gains on multiple reasoning benchmarks, including +86.2 on Sudoku, +51.6 on Countdown, +4.5 on GSM8K, and +5.3 on Math500. Ablation studies and computational cost analyses further demonstrate the effectiveness and practicality of our design choices.

1 Introduction

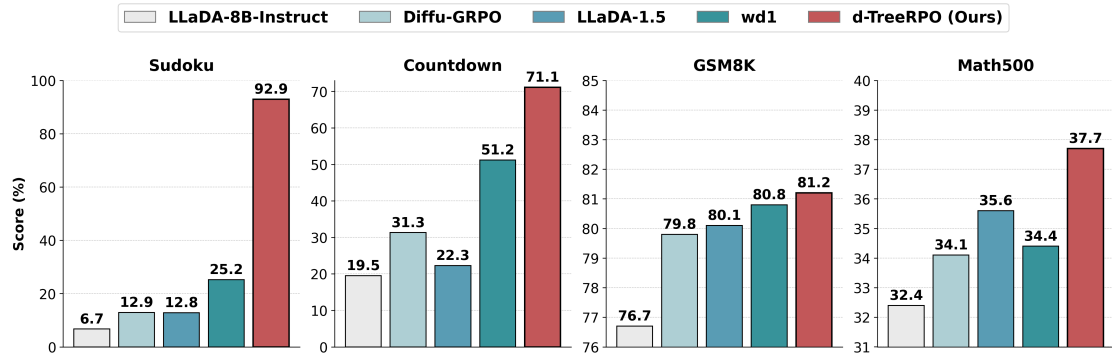


Figure 1: Performance comparison of *d*-TreeRPO with existing dLLM RL methods on four reasoning benchmarks. All methods are evaluated with a generation length of 256 in 128 denoising steps. All tasks adopt zero-shot evaluation with pass@1 scoring.

Diffusion large language models (dLLMs) (Nie et al., 2024; Ye et al., 2023; Zhang et al., 2025) provide a parallel decoding alternative to auto-regressive (AR) models. Unlike AR’s sequential

*This work is done during Leyi Pan’s internship at Tongyi Lab, Alibaba Group.

† Corresponding authors.

generation, dLLMs start with masked inputs and iteratively reveal tokens through parallel denoising steps, enabling faster inference. Closed-source models (e.g., Gemini Diffusion, Seed Diffusion (Song et al., 2025)) achieve 1,400-2,150 tokens/s, while open-source models like LLaDA (Nie et al., 2025; Zhu et al., 2025a,b), Dream (Ye et al., 2025; Xie et al., 2025b) and SDAR (Cheng et al., 2025) match or exceed AR models with comparable size in performance.

Reinforcement learning (RL) plays a pivotal role in enhancing dLLM reasoning capabilities (Zhao et al., 2025; Huang et al., 2025; Tang et al., 2025). Modern policy optimization algorithms such as PPO (Schulman et al., 2017) and GRPO (Shao et al., 2024) build upon the policy gradient framework, and their updates fundamentally rely on two core components: the advantage estimate A_t and the action log-probability $\log \pi_\theta(a_t | s_t)$. However, both of these components are prone to estimation errors, leading to suboptimal optimization outcomes. To ensure reliable RL for dLLMs, two requirements must be satisfied: **(1) granular and verifiable reward signals that ensure accurate advantage calculation, and (2) precise estimation of action log-probabilities.**

However, current dLLM RL approaches face significant limitations in both aspects. First, reward design lacks granularity or verifiability. Current approaches either rely solely on sparse outcome rewards (ignoring intermediate denoising steps) (Zhao et al., 2025; Tang et al., 2025; Wang et al., 2025a; Zhu et al., 2025a) or employ unverified process signals, such as uniform step-wise rewards broadcasted from final outcomes (Huang et al., 2025; Yang et al., 2025a) or model-predicted state rewards (Wang et al., 2025b) which is at the risk of reward hacking. Second, log-probability estimation remains fundamentally challenging due to dLLMs' any-order decoding nature. Unlike auto-regressive (AR) models that decompose sequences via the chain rule for exact probability computation in a single forward pass (Shao et al., 2024; Zheng et al., 2025; Yu et al., 2025), dLLMs require approximations. Existing log-probability estimation in dLLMs suffer from unanalyzed approximation errors. For instance, ELBO-based methods used in LLaDA (Nie et al., 2025) and MMaDA (Yang et al., 2025c) provide only a biased lower bound of the authentic log-probability, and necessitate costly multi-time forward passes to estimate the bound. While methods like Diffu-GRPO (Zhao et al., 2025) reduce computation by estimating ELBO through single-time forward pass, this simplification exacerbates the gap from the unbiased expectation.

To address these challenges, we propose *d*-TreeRPO, a more reliable policy optimization algorithm for diffusion language models. Our method organizes rollouts as trees, where leaf nodes correspond to terminal states with verifiable rewards (e.g., puzzle solutions or math answers). State rewards propagate upward through the tree hierarchy: the reward of a parent node R_{parent} is computed as the average of its children's rewards, i.e., $R_{\text{parent}} = \frac{1}{|C|} \sum_{c \in C} R_c$. Action advantages are then calculated as $A = R_{\text{child}} - R_{\text{parent}}$. This mechanism provides dense, verifiable process rewards grounded in actual sampling outcomes, mitigating reward hacking risks. To better estimate transition log-probability from parent nodes to child nodes, we theoretically establish that the error between single-time forward pass probability estimates and the unbiased expectation decreases as model confidence (determinism) increases. However, excessive determinism early in training restricts exploration (Li et al., 2025; Cui et al., 2025; Zhang et al., 2024; Tan et al., 2025), which forms a critical exploration-exploitation trade-off in dLLM RL. To reconcile this, we introduce a time-scheduled self-distillation loss implemented as a KL divergence constraint. This loss aligns the policy with a target distribution derived from advantage-weighted voting over positive advantage samples. During early training phases, the constraint is relaxed to encourage diverse exploration; its influence gradually strengthens to sharpen determinism, improving transition probability estimation and final convergence (see Section 3.4 for details).

We conducted extensive experiments to validate the effectiveness of *d*-TreeRPO. Results show that models trained using *d*-TreeRPO on LLaDA-8B-Instruct outperform baselines across multiple datasets, including Sudoku, Countdown, GSM8k (Cobbe et al., 2021), and Math500 (Lightman et al., 2023), as shown in Figure 1. To further verify the effectiveness of the self-distillation loss, we performed comprehensive ablation studies comparing performance with and without the self-distillation loss, as well as alternate designs such as increasing diversity or applying reverse time schedule. The study demonstrates that the progressively stronger self-distillation loss design during training is effective and beneficial. In summary, our key contributions include:

- We propose *d*-TreeRPO, a more reliable policy optimization algorithm for diffusion language models, which provides fine-grained and verifiable rewards and more reliable probability estimations.
- We theoretically show that the error in estimating transition log-probabilities from parent to child nodes decreases as the model’s predictions become more confident, and reveal the exploration-exploitation trade-off in dLLM RL. Based on this, we propose a time-scheduled self-distillation loss to relieve the trade-off and ensure better convergence.
- Experiments show that *d*-TreeRPO achieves significant improvements on several reasoning benchmarks, including **+86.2 on Sudoku**, **+51.6 on Countdown**, **+4.5 on GSM8k**, and **+5.3 on Math500**. Meanwhile, comprehensive ablation studies and computational cost analyses further demonstrate the effectiveness of self-distillation loss and *d*-TreeRPO’s practicality.

2 Preliminaries

Diffusion Large Language Models. dLLMs generate text through an any-order denoising process, gradually reconstructing masked tokens into meaningful text until completing the generation (Ye et al., 2023; Nie et al., 2025). During training, for a randomly selected denoising step $t \in [0, 1]$, tokens in the training corpus are masked with a probability α_t , where α_t decreases progressively as t increases. The model then predicts the original tokens at masked positions by leveraging bidirectional attention. During inference, given a prompt q and a target generation length L , the model begins by initializing the completion as a fully masked sequence $\{[\text{MASK}]\}^L$ at step $t = 1$. Starting with $z_1 = [q; \{[\text{MASK}]\}^L]$, the model first predicts token distributions for all positions through a single-time forward pass f_θ . It then selects a subset of tokens (e.g., the top- k most confident tokens in masked positions) to unmask via sampling, updates the state to $z_{1-\Delta t}$, and proceeds to the next denoising step. This process of forward prediction and sampling is repeated until completion through multiple denoising steps.

Group Relative Policy Optimization and its use in dLLMs. GRPO (Shao et al., 2024) extends PPO (Schulman et al., 2017) with group-relative advantage estimation. The training objective is:

$$\mathcal{J}_{\text{GRPO}}(\theta) = \mathbb{E}_{\substack{q \sim \mathcal{D}, \\ o_1, \dots, o_G \sim \pi_{\theta_{\text{old}}}(\cdot | q)}} \left\{ \frac{1}{G} \sum_{i=1}^G \frac{1}{|o_i|} \sum_{k=1}^{|o_i|} [\min(r_{i,k}(\theta) A_{i,k}, \text{clip}(r_{i,k}(\theta), 1 - \epsilon, 1 + \epsilon) A_{i,k}) - \beta \mathcal{D}_{\text{KL}}(\pi_\theta \| \pi_{\text{ref}})] \right\}, \quad (1)$$

where $\{o_i\}_{i=1}^G$ is a group of G trajectories drawn from the old policy, group-relative advantage $A_{i,k} = \frac{R_{i,k} - \text{mean}(\{R_{i,k}\}_{i=1}^G)}{\text{std}(\{R_{i,k}\}_{i=1}^G)}$, and importance sampling ratio $r_{i,k}(\theta) = \frac{\pi_\theta(o_i^k | q, o_i^{<k})}{\pi_{\theta_{\text{old}}}(o_i^k | q, o_i^{<k})}$. For dLLMs, computational efficiency dictates that we typically do not optimize at every individual denoising step, because each step requires a full forward pass over all positions. Instead, we treat the transition from a fully masked input to a complete output as a single state transition (Zhao et al., 2025), or we partition it into a small number of large steps (Wang et al., 2025b). Under this training objective and the specifics of dLLMs, two factors are crucial for reliable dLLM RL: 1) *accurate advantage estimation*, including verifiable and fine-grained discrimination of the quality of state transitions, and 2) *precise estimation of the probability of a given state transition*. In AR models, the probability is straightforward due to sequential factorization: $\pi_{\text{AR}}(y_i | q) = \prod_{j=1}^{|y_i|} \pi(y_i^j | y_i^{<j}, q)$, where y_i refers to the trajectory o_i ’s final completion. In dLLMs, however, diverse decoding orders break this simple factorization, necessitating an expectation over all denoising paths: $\pi_{\text{dLLM}}(y_i | q) = \mathbb{E}_{\sigma \sim \Omega} \left[\prod_{k=1}^T \pi(z_{t_{k-1}} | z_{t_k}) \right]$, where σ is a permutation of unmasking orders during the generation of y_i , z_{t_T} the initial state ($t_T = 1$), and z_{t_0} the final state ($t_0 = 0$).

Existing dLLM RL Methods. While existing works attempt to address the aforementioned two aspects, critical limitations remain.

1) *Reward/Advantage calculation and assignment*: Approaches like Diffu-GRPO (Zhao et al., 2025), wd1 (Tang et al., 2025), and d2 (Wang et al., 2025a) rely solely on outcome rewards for training, ignoring intermediate denoising steps. SAPO (Xie et al., 2025a) add a process-aware reward to the final outcome reward, but still optimizes the whole trajectory from fully masked to fully

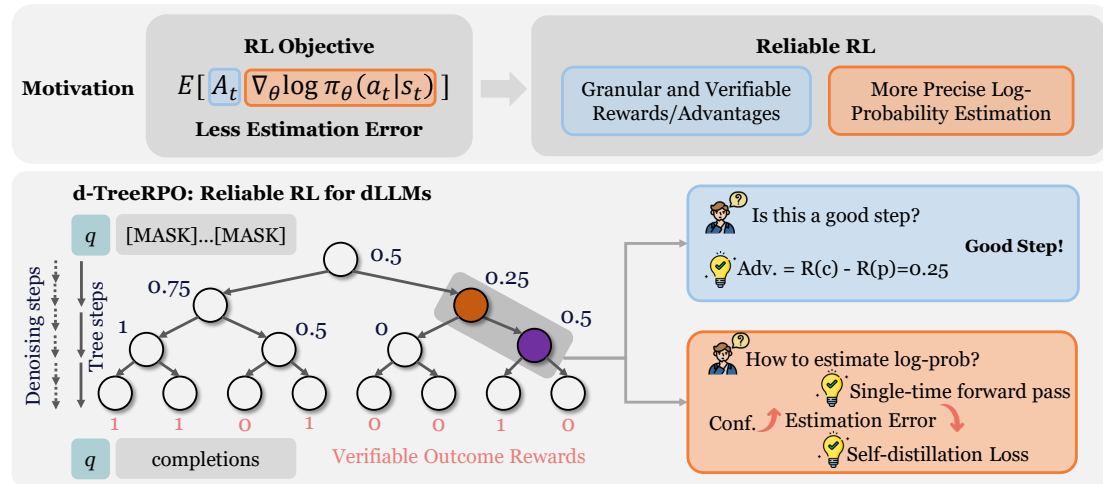


Figure 2: Overview of our proposed d -TreeRPO. By analyzing the RL objective, we identify two requirements for reliable policy optimization: granular/verifiable advantage signals and precise log-probability estimation. Our framework employs a tree-structured rollout that propagates verifiable outcome rewards bottom-up through the denoising hierarchy to establish verifiable step-wise advantages, coupled with single-time forward pass estimation of parent-to-child transition log-probabilities. Guided by theoretical analysis of prediction confidence errors, we further introduce a time-scheduled self-distillation mechanism that progressively sharpens model determinism in later training stages, ensuring more precise estimation and better convergence.

decoded and therefore lacks fine-grained reward assignment. CJ-GPRO (Yang et al., 2025a) and DCOLT (Huang et al., 2025) assign the same final reward to all steps, lacking step-specific signals. TraceRL (Wang et al., 2025b) employs a value model to predict per-state rewards for finer granularity, but its reliance on unverified intermediate rewards introduces risks of reward hacking. **Fundamentally, reward design in existing dLLM RL methods cannot achieve both granularity and verifiability, leading to errors in advantage estimation.**

2) *Prediction probability estimation:* Methods like LLaDA and MMaDA estimate $\log \pi_\theta(y|q)$ using the evidence lower bound (ELBO): $\log \pi_\theta(y|q) \geq \mathbb{E}_{t, z_t} \left[\sum_{k=1}^{|y|} w(t) \cdot \mathbb{1}(z_{t,k} = [\text{MASK}]) \cdot \log f_\theta(y^k | z_t, q) \right]$, where z_t denotes the state at denoising step t , $w(t)$ the time-dependent weight and f_θ the model’s forward function. While ELBO provides a tractable objective, it yields a biased lower-bound estimate and requires computationally expensive multi-time masking/forward passes for accuracy. For efficiency, Diffu-GRPO (Zhao et al., 2025) approximates ELBO using a single forward pass on fully masked completions, exacerbating estimation bias. VRPO (LLaDA-1.5) (Zhu et al., 2025a) reduces variance via 8 forward passes initialized from distinct decoding timesteps. d2-stepMerge (Wang et al., 2025a) estimates probabilities by multiplying conditional transition probabilities across multiple denoising steps. **However, none of these methods rigorously quantify the bias between their approximations and the unbiased expected prediction probability $\mathbb{E}_{\sigma \sim \Omega} \left[\prod_{k=1}^T \pi(z_{t_{k-1}} | z_{t_k}) \right]$ that accounts for all decoding orders, undermining the reliability of policy gradient updates.**

3 d -TreeRPO: Towards More Reliable Policy Optimization for dLLMs

We present d -TreeRPO, a policy optimization framework that enhances reliability of dLLM RL by providing granular and verifiable reward design and precise log-probability estimation. As depicted in Figure 2, our approach begins with the tree-structured reinforcement learning mechanism (Section 3.1) that decomposes denoising trajectories into hierarchical steps, enabling step-specific, verifiable rewards via bottom-up reward calculation. Next, we estimate conditional

transition log-probabilities between parent-child nodes via a single-time forward pass (Section 3.2). To ensure reliability, we establish theoretical bounds (Section 3.3) on the estimation error between our approximation and the unbiased expected probability, proving that higher prediction confidence reduces this error. Building on this insight, we design a time-scheduled self-distillation loss (Section 3.4) to enhance prediction determinism in later training stages, thereby minimizing estimation error and improving convergence. Finally, we formalize the complete d -TreeRPO loss function and present its end-to-end training workflow (Section 3.5).

3.1 Tree-Structured RL: Constructing Granular and Verifiable Rewards

Tree-Structured Rollout. To reduce computational costs during rollout, we introduce a merging parameter s , which groups the N denoising steps of dLLM into N/s groups, with each group forming a tree step. Thus, the path from the root to the leaf consists of $H = N/s$ tree steps. For each tree node except the leaf nodes, B independent samplings are performed, where each independent sampling involves s consecutive diffusion steps. The sampling principle follows the inherent sampling mechanism of the dLLM being trained, such as confidence-based sampling in LLaDA (where the total generation length L and denoising steps N are hyper-parameters, and each denoising step decodes the top- L/N tokens with the highest confidence in that step's forward pass) (Nie et al., 2025). Such tree construction results in B^H leaf nodes for the same prompt, corresponding to B^H complete completions.

Rewards and Advantages. The reward for each leaf node is determined by the verifiable outcome rewards. Based on this, the state reward of each tree node is computed bottom-up as the average of the state rewards of its child nodes, i.e.,

$$R_p = \frac{1}{|C_p|} \sum_{c \in C_p} R_c, \quad (2)$$

where C_p is the set of child nodes of node p and R_c is the reward of child node c . The transition advantage from a parent node to a child node is defined as:

$$A_p^c = R_c - R_p = R_c - \frac{1}{|C_p|} \sum_{c' \in C_p} R_{c'}, \quad (3)$$

where the child nodes under the same parent node are treated as a group, and the relative advantage is calculated within this group.

Optimization Overview. During training, we treat one tree step as a state transition and perform group-wise policy updates over each parent's child set C_p , using a clipped-ratio objective augmented with a KL penalty relative to a reference policy. This requires the conditional transition probability ratio $\frac{\pi_\theta(c|p)}{\pi_{\theta_{old}}(c|p)}$ and the group-relative advantage A_p^c . Since dLLMs' any-order decoding makes these conditional probabilities intractable to compute exactly, we provide a single-time forward pass approximation and the corresponding trainable objective in Sec. 3.2.

3.2 Estimation of Conditional Log-Probabilities in Tree Structures

Single-time Forward Pass Estimation. Following Diffu-GRPO (Zhao et al., 2025), we utilize the sum of log-probabilities in a single-time forward pass to estimate the conditional transition log-probabilities between parent and child nodes. Suppose the positions newly decoded in the child node compared to its parent are d_1, d_2, \dots, d_k , with the corresponding tokens $y^{d_1}, y^{d_2}, \dots, y^{d_k}$. Then the estimation is as follows:

$$\log \hat{\pi}_\theta(c | p) = \sum_{i=1}^k \log f_\theta^{d_i}(y^{d_i} | p), \quad (4)$$

where $\log \hat{\pi}_\theta(c | p)$ denotes the estimation of $\log \pi_\theta(c | p)$, and $f_\theta^{d_i}$ represents the distribution of model's forward function at position d_i . p corresponds to the parent node's state, which includes the prompt and the partially masked completion.

Vanilla d -TreeRPO Loss. Therefore, The GRPO-like loss using tree-structured RL and single-time forward pass estimation is as follows:

$$\mathcal{L}_{\text{vanilla-}d\text{-TreeRPO}}(\theta) = -\mathbb{E}_{q \sim \mathcal{D}, p \in \mathcal{T}(q)} \left[\frac{1}{|C_p|} \sum_{c \in C_p} \frac{1}{k} \sum_{i=1}^k \left(\min \left(\frac{f_\theta^{d_i}(y^{d_i} | p)}{f_{\theta_{old}}^{d_i}(y^{d_i} | p)} A_p^c, \text{clip} \left(\frac{f_\theta^{d_i}(y^{d_i} | p)}{f_{\theta_{old}}^{d_i}(y^{d_i} | p)}, 1 - \epsilon, 1 + \epsilon \right) A_p^c \right) - \beta D_{\text{KL}} [\pi_\theta(\cdot | p) || \pi_{\text{ref}}(\cdot | p)] \right) \right]. \quad (5)$$

Comparability Issue and Block-wise Adaptation. The design described above introduces a comparability issue: when child nodes of the same parent decode different positions within the same tree step, the log-probabilities estimated by Equation (4) become incomparable across child nodes. In dLLM inference, a **block-wise** decoding approach is often employed to achieve better performance. For a target generation length L , total denoising steps N , and block length b , each block undergoes $\frac{bN}{L}$ denoising steps. Within each block, tokens can be decoded in any order, while the blocks themselves are processed sequentially, forming a semi-autoregressive decoding framework. Therefore, we can resolve the comparability issue by aligning the tree-search hyper-parameters with this block-wise structure. Specifically, we ensure that the total number of tree steps H (from root to leaf) divides the number of blocks, i.e., L/b . This guarantees that each tree step decodes entire blocks, so that all child nodes of the same parent decode exactly the same set of positions (although the decoding order may vary across different denoising steps within a tree step), thereby restoring comparability of the log-probabilities among sibling nodes.

3.3 Theoretical Analysis: Relationship Between Prediction Confidence and Estimation Error

In this section, we analyze the approximation error between the single-step forward product probability $\hat{P}(c | p)$ and the unbiased s -step transition expected probability $P(c | p)$, proving that increasing prediction confidence reduces estimation error.

Notations and Setup. Let p denote the parent state (partially decoded tokens with masks) and c a child state generated through the continued s denoising steps (a tree step). Each tree step decodes k tokens. Let $\sigma = (\sigma_1, \dots, \sigma_k)$ be the true revelation order, where σ_t denotes the position revealed at step t . For notational simplicity, we assume one token is decoded per step, hence $t \in [1, k]$. The generation strategy follows distribution $\mathcal{Q}(\sigma)$ over possible orders Ω , with $\sum_{\sigma \in \Omega} \mathcal{Q}(\sigma) = 1$. Let $f_\theta^j(\cdot | \text{ctx})$ denote the distribution of model θ 's forward function at position j , giving context ctx .

Unbiased Transition Probability. Let $q_t(\sigma)$ denotes the probability of predicting the target token y^{σ_t} at decoding step t for order σ :

$$q_t(\sigma) = f_\theta^{\sigma_t}(y^{\sigma_t} | p, \{y^{\sigma_1}, \dots, y^{\sigma_{t-1}}\}, [\text{MASK}]_{\text{else where}}), \quad (6)$$

where the context for step t consists of parent state p , tokens decoded in earlier steps of current tree step $\{y^{\sigma_1}, \dots, y^{\sigma_{t-1}}\}$, and positions remaining masked in current step $[\text{MASK}]_{\text{else where}}$. Thus, the actual s -step transition probability is:

$$P(c | p) = \mathbb{E}_{\sigma \sim \mathcal{Q}(\sigma)} \left[\prod_{t=1}^k q_t(\sigma) \right]. \quad (7)$$

Single-time Forward Pass Estimation. Our method estimates the transition probability via single-time forward pass:

$$\hat{P}(c | p) = \prod_{j=1}^k f_\theta^j(y^j | p). \quad (8)$$

Definition of Confidence Gap. Define the parent-state per-position probabilities $f_j^* = f_\theta^j(y^j | p)$ and the path-wise per-step probabilities $q_t(\sigma)$ as above. Let

$$\epsilon_{\text{parent}} = \max_{1 \leq j \leq k} (1 - f_j^*), \quad \epsilon_{\text{path}} = \sup_{\sigma \in \Omega, 1 \leq t \leq k} (1 - q_t(\sigma)), \quad (9)$$

and define a most-uncertain-step confidence gap: $\epsilon = \max \{\epsilon_{\text{parent}}, \epsilon_{\text{path}}\}$

Estimation Error Bounds. With the above definition of ϵ , the following bounds hold:

$$(1 - \epsilon)^k \leq \frac{P(c \mid p)}{\hat{P}(c \mid p)} \leq \exp\left(\frac{k\epsilon}{1 - \epsilon}\right) \quad (10)$$

In particular, as $\epsilon \rightarrow 0$, using Taylor expansion,

$$\boxed{1 - k\epsilon + O(\epsilon^2) \leq \frac{P(c \mid p)}{\hat{P}(c \mid p)} \leq 1 + k\epsilon + O(\epsilon^2)} \quad (11)$$

and the approximation ratio converges to 1, showing that higher prediction confidence (smaller ϵ) yields smaller estimation error. The detailed proof is provided in Appendix A.

3.4 Design of Self-distillation Loss

Exploration-Exploitation Trade-off in dLLM RL. Based on the analysis in Section 3.3, higher prediction confidence improves the accuracy of log-probability estimation. However, this increased certainty inherently limits the model’s exploration during rollouts (Cui et al., 2025; Zhang et al., 2024), creating a inherent trade-off in dLLM reinforcement learning. During early training stages, exploration capability proves crucial for effective learning, while precise probability estimation becomes increasingly vital in later phases to ensure stable convergence toward high-value regions. Therefore, we propose a **time-scheduled self-distillation loss**: starting with minimal weighting to encourage early exploration, it progressively increases throughout training. This mechanism allows the model to gradually shift from broad exploration to sharper focus on high-advantage actions as training advances. The specific design is as follows:

Advantage-Weighted Target Distribution. For a depth-1 subtree, we first select child nodes with positive advantages $C_p^+ = \{c \in C_p \mid A_p^c > 0\}$. The time-dependent temperature $\tau(t)$ controls distribution sharpness:

$$\tau(t) = \tau_{\max} \cdot \left(1 - \frac{t}{T}\right)^\beta, \quad (\beta \in (0, 1]) \quad (12)$$

where T denotes total training steps, and t is the current training step. The advantage-weighted coefficients are computed through:

$$w_c = \frac{\exp\left(A_p^c / \tau(t)\right)}{\sum_{c' \in C_p^+} \exp\left(A_p^{c'} / \tau(t)\right)}, \quad \forall c \in C_p^+ \quad (13)$$

For each position-token pair (σ_i, v) ($\sigma_1, \dots, \sigma_k$ are positions decoded in current tree step, and $v \in \mathcal{V}$, \mathcal{V} is the vocabulary set), we construct the target distribution $P_{\text{target}}^{\sigma_i}(v)$ through advantage-weighted aggregation:

$$P_{\text{target}}^{\sigma_i}(v) = \frac{\sum_{c \in C_p^+} w_c \cdot \mathbb{1}[v_c^{\sigma_i} = v]}{\sum_{c \in C_p^+} w_c}, \quad \forall v \in \mathcal{V} \quad (14)$$

Time-scheduled Self-distillation Loss. The final self-distillation loss is then defined as:

$$\mathcal{L}_{\text{distill}}(\theta) = \lambda(t) \cdot \mathbb{E}_{q \sim \mathcal{D}, p \in \mathcal{T}(q)} \left[\frac{1}{k} \sum_{i=1}^k D_{\text{KL}} \left(P_{\text{target}}^{\sigma_i}(\cdot) \parallel \pi_{\theta}^{\sigma_i}(\cdot | p) \right) \right], \quad (15)$$

where $\lambda(t) = \lambda_{\max} \cdot \frac{e^{\gamma t/T} - 1}{e^{\gamma} - 1}$ is a time-scheduled weight. As training progresses, $\tau(t)$ becomes increasingly sharp, favoring selections from child nodes with the highest advantages, while $\lambda(t)$ grows progressively larger, causing the self-distillation loss being increasingly important.

Algorithm 1 d -TreeRPO: Tree-based Relative Policy Optimization for dLLMs

Require: Reference model π_{ref} , prompt distribution \mathcal{D} , tree branching factor B , tree height H , number of inner updates μ .

- 1: Initialize policy $\pi_{\theta} \leftarrow \pi_{\text{ref}}$
- 2: **while** not converged **do** $\pi_{\theta_{\text{old}}} \leftarrow \pi_{\theta}$
- 3: Sample a prompt $q \sim \mathcal{D}$
 // Phase 1: Rollout and Reward Calculation
- 4: Construct a rollout tree $\mathcal{T}(q)$ using policy $\pi_{\theta_{\text{old}}}$ with H steps and branching factor B .
- 5: Compute rewards R_p and advantages A_p^c for all nodes/steps using Eq. (2) and (3).
- 6: // Phase 2: Policy Update
- 7: **for** gradient update iterations $n = 1, \dots, \mu$ **do**
- 8: Sample a parent-child group (p, C_p) from the generated tree $\mathcal{T}(q)$.
- 9: Compute the total loss $\mathcal{L}_{d\text{-TreeRPO}}(\theta)$ using Eq. (16).
- 10: Update policy π_{θ} by taking a gradient step on the loss.
- 11: **end for**
- 12: **end while**
- 13: **return** The optimized policy π_{θ} .

3.5 Summary: Complete Loss Function and Algorithm Description

Combining Equation (5) and (15), the total loss of d -TreeRPO is as follows:

$$\begin{aligned} \mathcal{L}_{d\text{-TreeRPO}}(\theta) = & \mathbb{E}_{q \sim \mathcal{D}, p \in \mathcal{T}(q)} \left[-\frac{1}{|C_p|} \sum_{c \in C_p} \frac{1}{k} \sum_{i=1}^k \left(\underbrace{\min \left(\frac{f_{\theta}^{d_i}(y^{d_i}|p)}{f_{\theta_{\text{old}}}^{d_i}(y^{d_i}|p)} A_p^c, \text{clip} \left(\frac{f_{\theta}^{d_i}(y^{d_i}|p)}{f_{\theta_{\text{old}}}^{d_i}(y^{d_i}|p)}, 1-\epsilon, 1+\epsilon \right) A_p^c \right)}_{\text{policy-gradient loss}} \right. \right. \\ & \left. \left. - \underbrace{\beta D_{\text{KL}} [\pi_{\theta}(\cdot | p) || \pi_{\text{ref}}(\cdot | p)]}_{\text{KL loss}} \right) + \underbrace{\frac{\lambda(t)}{k} \sum_{i=1}^k D_{\text{KL}} \left(P_{\text{target}}^{\sigma_i}(\cdot) || \pi_{\theta}^{\sigma_i}(\cdot | p) \right)}_{\text{self-distillation loss}} \right]. \end{aligned} \quad (16)$$

The complete workflow of our proposed d -TreeRPO reinforcement learning algorithm is presented in Algorithm 1.

4 Experiments

In this section, we empirically validate the effectiveness of d -TreeRPO by answering the following research questions:

1. How does d -TreeRPO compare to existing RL algorithms for dLLMs in enhancing the reasoning capabilities of the base model? (Section 4.2)
2. How do the tree height H and branch factor B influence the performance of d -TreeRPO? (Section 4.3)
3. Does the self-distillation loss in d -TreeRPO contribute positively to training by improving the model's prediction confidence? (Section 4.4)
4. Is the temporal scheduling design, which gradually increases the self-distillation loss weight while sharpening the target distribution during training, effective and well-grounded? (Section 4.5)
5. What is the practicality of d -TreeRPO in terms of computational resource consumption and training time? (Section 4.6)

Table 1: Performance comparison of *d*-TreeRPO with existing dLLM RL methods across reasoning tasks under 256/512-token generation settings. Methods marked with \dagger use our re-implementations due to unavailable source code; others employ official codebases. Best results are **bolded**, with performance gains relative to the base model shown in parentheses.

Methods / Datasets	Sudoku		Countdown		GSM8k		Math500	
	256	512	256	512	256	512	256	512
LLaDA-8B-Instruct	6.7 (+0.0)	5.5 (+0.0)	19.5 (+0.0)	16.0 (+0.0)	76.7 (+0.0)	78.2 (+0.0)	32.4 (+0.0)	36.2 (+0.0)
+ Diffu-GRPO (Zhao et al., 2025)	12.9	11.2	31.3	37.1	79.8	81.9	34.1	39.0
+ VRPO (LLaDA-1.5) (Zhu et al., 2025a)	12.8	9.6	22.3	18.0	80.1	81.5	35.6	34.8
+ wd1 (Tang et al., 2025)	25.2	24.2	51.2	46.1	80.8	82.3	34.4	39.0
+ SAPO \dagger (Xie et al., 2025a)	20.3	16.1	52.0	56.3	80.6	82.1	33.8	38.4
+ d2-stepMerge \dagger (Wang et al., 2025a)	76.1	66.2	52.4	52.1	81.1	82.0	34.4	38.5
+ TraceRL (Wang et al., 2025b)	25.6	25.4	50.4	52.6	80.3	82.4	35.6	39.1
+ <i>d</i> -TreeRPO (ours)	92.9 (+86.2)	80.3 (+74.8)	71.1 (+51.6)	62.1 (+46.1)	81.2 (+4.5)	82.6 (+3.6)	37.7 (+5.3)	38.9 (+2.7)

4.1 Experimental Setup

Models and Datasets. We employ LLaDA-8B-Instruct (Nie et al., 2025) as the base model, which has undergone supervised fine-tuning but not reinforcement learning. For training and evaluation, we utilize two puzzle-based reasoning tasks: Sudoku and Countdown, and two mathematical reasoning tasks: GSM8K (Cobbe et al., 2021) and Math500 (Lightman et al., 2023). Following previous works (Zhao et al., 2025; Tang et al., 2025), we adopt the 4 \times 4 Sudoku training and test sets provided by Diffu-GRPO (Zhao et al., 2025) for Sudoku. For Countdown, models are trained on the 3to4 Countdown task training set¹ and evaluated using the test set provided by Diffu-GRPO. For GSM8K² and Math500³, we strictly follow their official training-test splits for both training and evaluation.

Baselines. We compare *d*-TreeRPO with multiple DLM RL baselines, including Diffu-GRPO (Zhao et al., 2025), VRPO (LLaDA-1.5) (Zhu et al., 2025a), wd1 (Tang et al., 2025), SAPO (Xie et al., 2025a), d2-stepMerge (Wang et al., 2025a) and TraceRL (Wang et al., 2025b).

Training Details. Following Diffu-GRPO (Zhao et al., 2025) and wd1 (Tang et al., 2025), we use LoRA during training with rank $r = 128$ and scaling factor $\alpha = 64$. We adopt a learning rate of 3×10^{-5} , set $\tau_{\max} = 2$ and $\beta = 0.7$ in Equation 12, and set $\lambda_{\max} = 3 \times 10^{-3}$ in self-distillation loss. The maximum generation length is configured as 256 tokens with block-wise decoding (block length= 32) over 128 denoising steps. To balance computational efficiency and training stability, our tree-structured rollout employs depth $H = 2$ and branch factor $B = 4$ (see Section 4.3 for sensitivity analysis). All experiments are conducted on 8 \times H20 GPUs.

Evaluation Details. We evaluate model performance under two generation settings: 256-token and 512-token outputs, with block-wise decoding (block length= 32) and deterministic sampling (temperature= 0.0). Denoising steps are configured as half the generation length (128 steps for 256-token generations; 256 steps for 512-token generations). All tasks adopt zero-shot evaluation with pass@1 scoring.

4.2 Main Results

Table 1 compares *d*-TreeRPO with existing dLLM RL methods. Our method achieves state-of-the-art performance across most settings, demonstrating significant gains over the base model: +86.2% on Sudoku, +51.6% on Countdown, +4.5% on GSM8K, and +5.3% on Math500 with 256-token generations. We observe task-dependent sensitivity to the length of generated outputs:

¹<https://huggingface.co/datasets/Jiayi-Pan/Countdown-Tasks-3to4>

²<https://huggingface.co/datasets/openai/gsm8k>

³train: <https://huggingface.co/datasets/ankner/math-500>, test: <https://huggingface.co/datasets/HuggingFaceH4/MATH-500>

tasks that do not require overly long chains of reasoning, such as Sudoku and Countdown, exhibit some degradation under the 512-token setting due to our conservative 256-token training limit. In contrast, tasks like GSM8K and Math500 benefit from extended generation capacity, as the additional tokens provide a structured space for multi-step reasoning and derivations.

4.3 Analysis of Tree Height H and Branch Factor B

Analysis of Tree Height H . The tree height H is defined as the number of steps required to traverse from the root node to a leaf node in the tree. Increasing the tree height H enables finer granularity in the generation trajectory, allowing for more precise reward assignment. Concurrently, as the number of tokens k generated per tree step decreases with higher tree heights, the probability estimation error reduces according to Equation (11). We compared the training curves using $H = 1, 2, 4$ over the first 30 training steps, as shown in Figure 3a. Results show that the curve for $H = 4$ rises the fastest, followed by $H = 2$, while $H = 1$ has the slowest improvement, aligning well with our analysis and further demonstrating the potential of d -TreeRPO. However, as the computational cost of d -TreeRPO grows exponentially with H , our available computing resources could not support the convergence of $H = 4$ within a reasonable training time (see Section 4.6 for details). Therefore, we ultimately chose $H = 2$ as the primary setting for our experiments, which already yields satisfactory performance.

Analysis of Branch Factor B . The branch factor B denotes the number of child nodes expanded from a parent node during rollout. A larger B increases the diversity of exploration and reduces the variance in the estimated state reward baseline for the parent node. We compared training curves using $B = 2, 4$, and 6, as shown in Figure 3b. The results indicate that on the Sudoku task, the policy trained with $B = 2$ achieves a final reward of only around 0.2, whereas both $B = 4$ and $B = 6$ converge to comparable performance levels above 0.9. Notably, $B = 6$ exhibits faster initial improvement than $B = 4$. However, as analyzed in Section 4.6, the computational cost grows polynomially with B . To balance training efficiency and performance, we adopt $B = 4$ as the primary setting for our experiments.

4.4 Effectiveness of Self-distillation Loss

To validate the effectiveness of our proposed self-distillation loss, we conduct comprehensive ablation studies. First, we compare the full d -TreeRPO model against a variant where the self-distillation loss is removed. Furthermore, to emphasize the importance of progressively sharpening the policy distribution, we design a contrasting objective which we term the **diversity-promoting loss** (\mathcal{L}_{div}). This loss is designed to be symmetric to $\mathcal{L}_{\text{distill}}$ but with an opposing goal: to intentionally increase policy diversity and reduce model confidence in later training stages. Drawing inspiration from prior work that suggests decreasing entropy for positive samples and increasing it for negative ones (Yang et al., 2025b), the diversity loss operates on nodes with negative advantages. Specifically, it selects child nodes from the set $C_p^- = \{c \in C_p \mid A_p^c < 0\}$ and computes weights based on the absolute value of their advan-

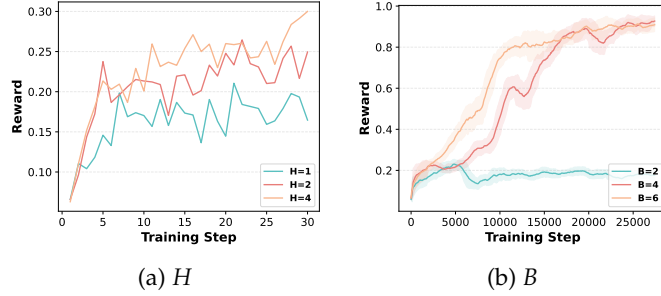


Figure 3: Training rewards on Sudoku task under different parameters H and B .

Figure 3b shows that $B = 6$ exhibits faster initial improvement than $B = 4$. However, as analyzed in Section 4.6, the computational cost grows polynomially with B . To balance training efficiency and performance, we adopt $B = 4$ as the primary setting for our experiments.

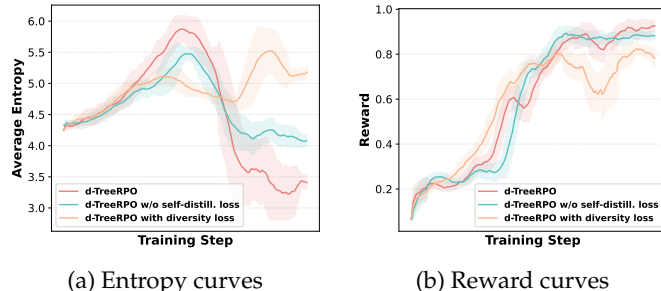


Figure 4: Training curves for the Sudoku task.

tages, $|A_p^c|$. A “negative” target distribution, $P_{\text{div-target}}$, is then constructed via weighted voting, mirroring the process for P_{target} . Finally, instead of minimizing the KL divergence, the policy is trained to actively move away from this undesirable distribution using a negative KL divergence objective, which shares the same time-scheduling coefficient $\lambda(t)$ as our primary loss:

$$\mathcal{L}_{\text{div}}(\theta) = -\lambda(t) \cdot \mathbb{E}_{q \sim \mathcal{D}, p \in \mathcal{T}(q)} \left[\frac{1}{k} \sum_{i=1}^k D_{\text{KL}} \left(P_{\text{div-target}}^{\sigma_i}(\cdot) \parallel \pi_{\theta}^{\sigma_i}(\cdot | p) \right) \right]. \quad (17)$$

This setup provides a direct comparison between the effects of time-scheduled policy sharpening (our method) and forced policy diversification.

Figure 4 plots the evolution of policy entropy and training reward for three settings on the Sudoku task: the standard d -TreeRPO, an ablation without self-distillation, and a counterpart trained with a diversity-promoting loss. As observed, the policy entropy for all three settings initially increases, a typical behavior corresponding to the exploration phase in early-to-mid reinforcement learning. However, their trajectories diverge in the later stages. The entropy of the model without self-distillation naturally begins to decline, indicating inherent policy convergence. Our proposed self-distillation loss significantly accelerates this decline, forcing the policy to become more confident and therefore reduce the estimation error. In stark contrast, the model with the diversity-promoting loss have the highest entropy in the later training process. Correspondingly, these distinct entropy behaviors are directly reflected in the reward curves. The model enhanced with self-distillation achieves the highest final reward, followed by the baseline without it. The diversity-focused variant not only yields the lowest final reward but also exhibits considerable instability during training.

Furthermore, we report the final evaluation performance of these three settings across all four tasks in Table 2. The results align with our training-time observations: the full d -TreeRPO algorithm consistently outperforms the other two variants. Removing the self-distillation loss leads to a noticeable drop in performance, while adding the diversity-promoting loss has the worst performance. These findings provide compelling evidence for the practical effectiveness of our proposed self-distillation loss in dLLM-based reinforcement learning.

Table 2: Comparison of evaluation performance of d -TreeRPO, d -TreeRPO without self-distillation loss and d -TreeRPO with diversity-promoting loss. The generation length is 256.

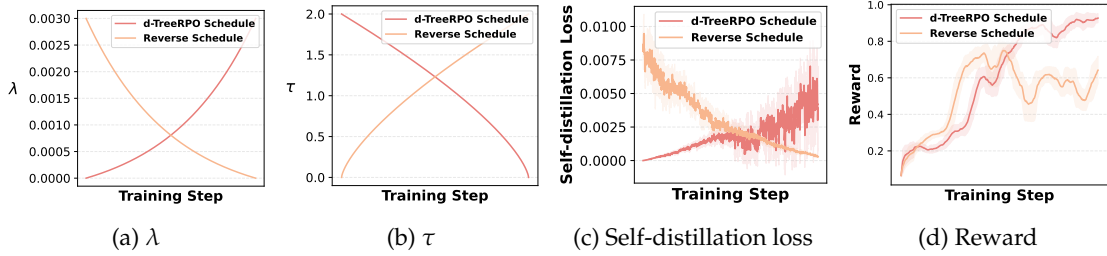
Method	Sudoku	Countdown	GSM8k	Math500
d -TreeRPO	92.9	71.1	81.2	37.7
d -TreeRPO w/o distill.	89.8	66.4	80.9	36.1
d -TreeRPO w. div.	84.2	63.4	78.5	35.2

4.5 Analysis of Time-scheduled Design of Self-distillation Loss

Comparison with Reverse-Scheduled Self-Distillation Loss. To validate the design choice of increasing $\lambda(t)$ and decreasing $\tau(t)$ during training in our self-distillation loss, we conducted experiments using a completely reversed scheduling strategy for $\lambda(t)$ and $\tau(t)$, termed *reverse-scheduled self-distillation*. Figure 5 illustrates the evolution of λ , τ , self-distillation loss, and reward over training steps for both the forward schedule (employed in d -TreeRPO) and the reverse schedule. As shown, under the reverse schedule, the self-distillation loss gradually decreases as training progresses. Initially, its reward curve rises even faster than that of d -TreeRPO. This occurs because the reverse-scheduled self-distillation loss is very large at the start, providing a strong distillation effect for the initially less capable model. However, as training continues and the reward reaches approximately 0.75, it begins to decline. This indicates that relying solely on distillation while suppressing exploration leads to insufficient generalization capability in the mid-to-late stages of training, demonstrating limited efficacy. This comparative analysis highlights the rationale behind the time-dependent schedule used in d -TreeRPO.

4.6 Computational Overhead

Analysis of Computational Overhead for d -TreeRPO. The computational overhead of the d -TreeRPO algorithm is primarily attributed to two components: (1) the rollout phase and (2) the loss computation and gradient updates. For the rollout phase, given the tree height H and the branch factor B , the total number of tree steps in a tree expanded from a single prompt is:

Figure 5: Training dynamics comparison: *d*-TreeRPO vs. its reverse-scheduled variant.

$\sum_{i=1}^H B^i = \frac{B(B^H-1)}{B-1}$. If a complete generation contains N denoising steps, then each tree step involves N/H denoising steps. Therefore, the total number of denoising steps for constructing a single tree is: $\left(\frac{B(B^H-1)}{B-1}\right) \cdot \frac{N}{H}$. During the loss computation and gradient update stage, we utilize a single-time forward pass to compute the transition probabilities between tree steps. As a result, a tree expanded from a single prompt requires a total of $\frac{B(B^H-1)}{B-1}$ forward passes. To reduce memory usage, we compute the loss for only one subtree at a time during each update.

Comparison of the Required Training Time with Other dLLM RL Methods. To demonstrate the practicality of our proposed *d*-TreeRPO method, we compared the training time required by *d*-TreeRPO against other dLLM RL baselines under the same GPU configuration ($8 \times$ H20 GPUs). Table 3 presents the training time required by these methods on the Sudoku task for processing the same amount of data (one batch, with per-device train batch size = 4), the average training time per parameter update given the same gradient accumulation setting, and the total training time needed to reach convergence. It can be observed that among all methods, *d*-TreeRPO demonstrates moderate training time, slower than Diffu-GRPO and wd1, comparable to TraceRL, but faster than SAPO and d2-stepMerge. However, its final performance surpasses all other algorithms significantly, making it a practical and effective choice.

Table 3: Training time comparison between *d*-TreeRPO and other dLLM RL baselines on the Sudoku task. All methods are tested under $8 \times$ H20 GPUs.

	Diffu-GRPO	wd1	SAPO	d2-stepMerge	TraceRL	<i>d</i> -TreeRPO
Training one batch of data (s)	109	87	423	3456	604	598
Updating model parameters once (s)	9.08	7.25	35.25	288.00	43.14	9.96
Convergence (h)	≈ 24	≈ 24	≈ 72	> 72	≈ 48	≈ 48
Performance (%)	12.9	25.2	20.3	76.1	25.6	92.9

5 Conclusion

This paper introduced *d*-TreeRPO, a reliable reinforcement learning framework for diffusion large language models that addresses two core challenges: constructing granular, verifiable advantage signals and improving the precision of action probability estimation. By organizing rollouts as trees and propagating verifiable outcome rewards bottom-up, *d*-TreeRPO provides step-wise, hack-resistant advantages. We further analyzed the gap between single forward pass probability estimates and the unbiased expectation, showing that higher prediction confidence reduces estimation error, and leveraged this insight with a time-scheduled self-distillation loss that encourages exploration early and sharper determinism later. Empirically, *d*-TreeRPO significantly outperform baselines across reasoning tasks including Sudoku, Countdown, GSM8K, and Math500. Ablations confirm the importance of the self-distillation loss, and a cost analysis demonstrates that the method is practical relative to existing dLLM RL baselines.

References

Shuang Cheng, Yihan Bian, Dawei Liu, Yuhua Jiang, Yihao Liu, Linfeng Zhang, Wenhui Wang, Qipeng Guo, Kai Chen, Biqing Qi, et al. Sdar: A synergistic diffusion-autoregression paradigm for scalable sequence generation. *arXiv preprint arXiv:2510.06303*, 2025.

Karl Cobbe, Vineet Kosaraju, Mohammad Bavarian, Mark Chen, Heewoo Jun, Lukasz Kaiser, Matthias Plappert, Jerry Tworek, Jacob Hilton, Reiichiro Nakano, Christopher Hesse, and John Schulman. Training verifiers to solve math word problems. *arXiv preprint arXiv:2110.14168*, 2021.

Ganqu Cui, Yuchen Zhang, Jiacheng Chen, Lifan Yuan, Zhi Wang, Yuxin Zuo, Haozhan Li, Yuchen Fan, Huayu Chen, Weize Chen, et al. The entropy mechanism of reinforcement learning for reasoning language models. *arXiv preprint arXiv:2505.22617*, 2025.

Zemin Huang, Zhiyang Chen, Zijun Wang, Tiancheng Li, and Guo-Jun Qi. Reinforcing the diffusion chain of lateral thought with diffusion language models. *arXiv preprint arXiv:2505.10446*, 2025.

Xianzhi Li, Ethan Callanan, Xiaodan Zhu, Mathieu Sibue, Antony Papadimitriou, Mahmoud Mahfouz, Zhiqiang Ma, and Xiaomo Liu. Entropy-aware branching for improved mathematical reasoning. *arXiv preprint arXiv:2503.21961*, 2025.

Hunter Lightman, Vineet Kosaraju, Yura Burda, Harri Edwards, Bowen Baker, Teddy Lee, Jan Leike, John Schulman, Ilya Sutskever, and Karl Cobbe. Let's verify step by step. *arXiv preprint arXiv:2305.20050*, 2023.

Shen Nie, Fengqi Zhu, Chao Du, Tianyu Pang, Qian Liu, Guangtao Zeng, Min Lin, and Chongxuan Li. Scaling up masked diffusion models on text. *arXiv preprint arXiv:2410.18514*, 2024.

Shen Nie, Fengqi Zhu, Zebin You, Xiaolu Zhang, Jingyang Ou, Jun Hu, Jun Zhou, Yankai Lin, Ji-Rong Wen, and Chongxuan Li. Large language diffusion models. *arXiv preprint arXiv:2502.09992*, 2025.

John Schulman, Filip Wolski, Prafulla Dhariwal, Alec Radford, and Oleg Klimov. Proximal policy optimization algorithms. *arXiv preprint arXiv:1707.06347*, 2017.

Zhihong Shao, Peiyi Wang, Qihao Zhu, Runxin Xu, Junxiao Song, Xiao Bi, Haowei Zhang, Mingchuan Zhang, YK Li, Yang Wu, et al. Deepseekmath: Pushing the limits of mathematical reasoning in open language models. *arXiv preprint arXiv:2402.03300*, 2024.

Yuxuan Song, Zheng Zhang, Cheng Luo, Pengyang Gao, Fan Xia, Hao Luo, Zheng Li, Yuehang Yang, Hongli Yu, Xingwei Qu, et al. Seed diffusion: A large-scale diffusion language model with high-speed inference. *arXiv preprint arXiv:2508.02193*, 2025.

Hongze Tan, Jianfei Pan, Jinghao Lin, Tao Chen, Zhihang Zheng, Zhihao Tang, and Haihua Yang. Gtpo and grpoo-s: Token and sequence-level reward shaping with policy entropy. *arXiv preprint arXiv:2508.04349*, 2025.

Xiaohang Tang, Rares Dolga, Sangwoong Yoon, and Ilija Bogunovic. wd1: Weighted policy optimization for reasoning in diffusion language models. *arXiv preprint arXiv:2507.08838*, 2025.

Guanghan Wang, Yair Schiff, Gilad Turok, and Volodymyr Kuleshov. d2: Improved techniques for training reasoning diffusion language models. *arXiv preprint arXiv:2509.21474*, 2025a.

Yinjie Wang, Ling Yang, Bowen Li, Ye Tian, Ke Shen, and Mengdi Wang. Revolutionizing reinforcement learning framework for diffusion large language models. *arXiv preprint arXiv:2509.06949*, 2025b.

Shaoan Xie, Lingjing Kong, Xiangchen Song, Xinshuai Dong, Guangyi Chen, Eric P Xing, and Kun Zhang. Step-aware policy optimization for reasoning in diffusion large language models. *arXiv preprint arXiv:2510.01544*, 2025a.

Zhihui Xie, Jiacheng Ye, Lin Zheng, Jiahui Gao, Jingwei Dong, Zirui Wu, Xueliang Zhao, Shansan Gong, Xin Jiang, Zhenguo Li, et al. Dream-coder 7b: An open diffusion language model for code. *arXiv preprint arXiv:2509.01142*, 2025b.

Jingyi Yang, Guanxu Chen, Xuhao Hu, and Jing Shao. Taming masked diffusion language models via consistency trajectory reinforcement learning with fewer decoding step. *arXiv preprint arXiv:2509.23924*, 2025a.

Kai Yang, Xin Xu, Yangkun Chen, Weijie Liu, Jiafei Lyu, Zichuan Lin, Deheng Ye, and Saiyong Yang. Entropic: Towards stable long-term training of llms via entropy stabilization with proportional-integral control. *arXiv preprint arXiv:2511.15248*, 2025b.

Ling Yang, Ye Tian, Bowen Li, Xincheng Zhang, Ke Shen, Yunhai Tong, and Mengdi Wang. Mmada: Multimodal large diffusion language models. *arXiv preprint arXiv:2505.15809*, 2025c.

Jiacheng Ye, Zhihui Xie, Lin Zheng, Jiahui Gao, Zirui Wu, Xin Jiang, Zhenguo Li, and Lingpeng Kong. Dream 7b: Diffusion large language models. *arXiv preprint arXiv:2508.15487*, 2025.

Jiasheng Ye, Zaixiang Zheng, Yu Bao, Lihua Qian, and Quanquan Gu. Diffusion language models can perform many tasks with scaling and instruction-finetuning. *arXiv preprint arXiv:2308.12219*, 2023.

Qiying Yu, Zheng Zhang, Ruofei Zhu, Yufeng Yuan, Xiaochen Zuo, Yu Yue, Weinan Dai, Tiantian Fan, Gaohong Liu, Lingjun Liu, et al. Dapo: An open-source llm reinforcement learning system at scale. *arXiv preprint arXiv:2503.14476*, 2025.

Hanning Zhang, Pengcheng Wang, Shizhe Diao, Yong Lin, Rui Pan, Hanze Dong, Dylan Zhang, Pavlo Molchanov, and Tong Zhang. Entropy-regularized process reward model. *arXiv preprint arXiv:2412.11006*, 2024.

Lingzhe Zhang, Liancheng Fang, Chiming Duan, Minghua He, Leyi Pan, Pei Xiao, Shiyu Huang, Yunpeng Zhai, Xuming Hu, Philip S Yu, et al. A survey on parallel text generation: From parallel decoding to diffusion language models. *arXiv preprint arXiv:2508.08712*, 2025.

Siyan Zhao, Devaansh Gupta, Qin Qing Zheng, and Aditya Grover. d1: Scaling reasoning in diffusion large language models via reinforcement learning. *arXiv preprint arXiv:2504.12216*, 2025.

Chujie Zheng, Shixuan Liu, Mingze Li, Xiong-Hui Chen, Bowen Yu, Chang Gao, Kai Dang, Yuqiong Liu, Rui Men, An Yang, et al. Group sequence policy optimization. *arXiv preprint arXiv:2507.18071*, 2025.

Fengqi Zhu, Rongzhen Wang, Shen Nie, Xiaolu Zhang, Chunwei Wu, Jun Hu, Jun Zhou, Jianfei Chen, Yankai Lin, Ji-Rong Wen, et al. Llada 1.5: Variance-reduced preference optimization for large language diffusion models. *arXiv preprint arXiv:2505.19223*, 2025a.

Fengqi Zhu, Zebin You, Yipeng Xing, Zenan Huang, Lin Liu, Yihong Zhuang, Guoshan Lu, Kangyu Wang, Xudong Wang, Lanning Wei, et al. Llada-moe: A sparse moe diffusion language model. *arXiv preprint arXiv:2509.24389*, 2025b.

A Detailed Proof of Estimation Error Bounds

Notations and Setup. Let p denote the parent state (partially decoded tokens with masks) and c a child state generated through the continued s denoising steps (a tree step). Each tree step decodes k tokens. Let $\sigma = (\sigma_1, \dots, \sigma_k)$ be the true revelation order, where σ_t denotes the position revealed at step t . For notational simplicity, we assume one token is decoded per step, hence $t \in [1, k]$. The generation strategy follows distribution $\mathcal{Q}(\sigma)$ over possible orders Ω , with $\sum_{\sigma \in \Omega} \mathcal{Q}(\sigma) = 1$. Let $f_\theta^j(\cdot \mid \text{ctx})$ denote the distribution of model θ 's forward function at position j , giving context ctx .

Unbiased Transition Probability. Let $q_t(\sigma)$ denotes the probability of predicting the target token y^{σ_t} at decoding step t for order σ :

$$q_t(\sigma) = f_\theta^{\sigma_t}(y^{\sigma_t} \mid p, \{y^{\sigma_1}, \dots, y^{\sigma_{t-1}}\}, [\text{MASK}]_{\text{else where}}), \quad (18)$$

where the context for step t consists of parent state p , tokens decoded in earlier steps of current tree step $\{y^{\sigma_1}, \dots, y^{\sigma_{t-1}}\}$, and positions remaining masked in current step $[\text{MASK}]_{\text{else where}}$. Thus, the actual s -step transition probability is:

$$P(c \mid p) = \mathbb{E}_{\sigma \sim \mathcal{Q}(\sigma)} \left[\prod_{t=1}^k q_t(\sigma) \right] \quad (19)$$

Single-time Forward Pass Estimation. Our method estimates the transition probability via single-time forward pass:

$$\hat{P}(c \mid p) = \prod_{j=1}^k f_\theta^j(y^j \mid p). \quad (20)$$

Definition of Confidence Gap. Define the parent-state per-position probabilities $f_j^* = f_\theta^j(y^j \mid p)$ and the path-wise per-step probabilities $q_t(\sigma)$ as above. Let

$$\epsilon_{\text{parent}} = \max_{1 \leq j \leq k} (1 - f_j^*), \quad \epsilon_{\text{path}} = \sup_{\sigma \in \Omega, 1 \leq t \leq k} (1 - q_t(\sigma)), \quad (21)$$

and define a most-uncertain-step confidence gap: $\epsilon = \max \{\epsilon_{\text{parent}}, \epsilon_{\text{path}}\}$

Upper Bound Analysis. Let $\delta_t(\sigma) = q_t(\sigma) - f_{\sigma_t}^*$ be the probability increment at step t for order σ . We have: $\delta_t(\sigma) \leq 1 - f_{\sigma_t}^* \leq \max_j (1 - f_j^*) \leq \epsilon$.

The unbiased transition probability expands as:

$$P(c \mid p) = \sum_{\sigma \in \Omega} \mathcal{Q}(\sigma) \prod_{t=1}^k (f_{\sigma_t}^* + \delta_t(\sigma)) \quad (22)$$

$$\leq \sum_{\sigma \in \Omega} \mathcal{Q}(\sigma) \prod_{t=1}^k (f_{\sigma_t}^* + \epsilon) \quad (23)$$

$$= \prod_{j=1}^k (f_j^* + \epsilon) \quad (24)$$

Given that $\hat{P}(c \mid p) = \prod_{j=1}^k f_\theta^j(y^j \mid p) = \prod_{j=1}^k f_j^*$, the log-ratio of probabilities satisfies:

$$\log \frac{P(c \mid p)}{\hat{P}(c \mid p)} \leq \sum_{j=1}^k \log \left(1 + \frac{\epsilon}{f_j^*} \right) \quad (25)$$

Given that $f_j^* \geq 1 - \epsilon$, we have:

$$\log \frac{P(c \mid p)}{\hat{P}(c \mid p)} \leq k \log \left(1 + \frac{\epsilon}{1 - \epsilon} \right) \quad (26)$$

$$\leq \frac{k\epsilon}{1 - \epsilon} \quad (\text{using } \log(1 + x) \leq x) \quad (27)$$

Exponentiating gives the upper bound:

$$\frac{P(c \mid p)}{\hat{P}(c \mid p)} \leq \exp\left(\frac{k\epsilon}{1-\epsilon}\right) \quad (28)$$

Lower Bound Analysis. By definitions, $q_t(\sigma) \geq 1 - \epsilon$ for all σ, t . Hence, for any σ :

$$\prod_{t=1}^k q_t(\sigma) \geq (1 - \epsilon)^k \quad (29)$$

Taking expectation over σ ,

$$P(c \mid p) = \mathbb{E}_\sigma \left[\prod_{t=1}^k q_t(\sigma) \right] \geq (1 - \epsilon)^k \quad (30)$$

Since $\hat{P}(c \mid p) \leq 1$, we obtain:

$$\frac{P(c \mid p)}{\hat{P}(c \mid p)} \geq (1 - \epsilon)^k \quad (31)$$

Combined Bounds. Combining (28) and (31):

$$(1 - \epsilon)^k \leq \frac{P(c \mid p)}{\hat{P}(c \mid p)} \leq \exp\left(\frac{k\epsilon}{1-\epsilon}\right) \quad (32)$$

As $\epsilon \rightarrow 0$, Taylor expanding reveals:

$$1 - k\epsilon + O(\epsilon^2) \leq \frac{P(c \mid p)}{\hat{P}(c \mid p)} \leq 1 + k\epsilon + O(\epsilon^2)$$

(33)

Conclusion. The approximation ratio converges to 1 as $\epsilon \rightarrow 0$, proving that higher prediction confidence (smaller ϵ) reduces estimation error.